Electronic Supplementary Material (ESI) for Journal of Materials Chemistry A

Supplementary Information for:

A copper-containing oxytelluride as a promising thermoelectric material for waste heat recovery

Paz Vaqueiro,[*a] Gabin Guelou,[a] Maria Stec,[a] Emmanuel Guilmeau[b] and Anthony V. Powell[a]

[a] Institute of Chemical Sciences & Centre for Advanced Energy Storage and Recovery (*CAESAR*), Heriot-Watt University, Edinburgh EH14 4AS, UK

[b] Laboratoire CRISMAT, UMR 6508 CNRS/ENSICAEN, 6 bd. du Maréchal Juin, F-14050 CAEN Cedex 4-France

1. Experimental Details

a) Synthesis of $Bi_{1-x}Pb_xOCuTe$

Stoichiometric mixtures of Cu, Te, Bi, α-Bi_2O_3 and PbO_2 were finely ground prior to be sealed in evacuated silica tubes (10^{-4} torr). Each mixture was first heated up to 350ºC with a ramp rate of 1°C min^{-1}. After 24 hours, the temperature was increased to 500ºC, and the silica tube maintained at that temperature for 48 hours. After slowly cooling down the tube to room temperature, each sample was ground and sealed in an evacuated silica tube again for a final firing at 500ºC for 72 hours. All samples are of high purity, and contain only trace amounts of Bi_2O_3 or Bi_2TeO_5. For electronic and thermal transport measurements, the as-prepared powders were hot pressed into well-densified pellets (~95% of theoretical density), at 773 K and 50 bar for 30 minutes under a N_2 flow. X-ray diffraction data collected on the hot-pressed pellets is consistent with the absence of texture, indicating that grains are randomly oriented.

b) Structural characterization

Samples were analysed by powder X-ray diffraction using a Bruker D8 Advance Powder X-ray diffractometer, operating with germanium monochromated $CuK_{\alpha 1}$ radiation (λ = 1.54046 Å) and fitted with a LynxEye detector. Data were collected over a range of $5 \leq 2\theta/^{o} \leq 120$ for a period of 10 hours. Rietveld refinements were carried out using the GSAS software.[1] The initial structural model was that of BiOCuTe, reported by Hiramatsu *et al.*[2]

c) Physical properties

Thermogravimetric analysis

Thermogravimetric analysis was performed using a DuPont Instruments 951 thermal analyser. Approximately 20 mg of finely ground crystals was heated under a flow of O_2 or N_2 over the temperature range $30 \leq T/°C \leq 600$ using a heating rate of 5°C min^{-1}.

Low temperature electrical conductivity

The electrical conductivity of the sample as a function of temperature was measured using a 4-probe DC technique. An ingot (~10 × 4 × 1 mm^3) was cut from a hot-pressed pellet, four 50 μm silver wires were attached using colloidal silver paint and connections were made to a Keithley 2182 nanovoltmeter and a TT*i* QL564P power supply. The sample was mounted in an Oxford Instruments CF1200 cryostat connected to an ITC502 temperature controller. Measurements were carried out over the temperature range $100 \leq T/K \leq 350$.

Low temperature Seebeck coefficient

Measurements of the Seebeck coefficient in 5K steps over the temperature range $100 \leq T/K \leq 300$ were made on ingots (ca. 7 × 3 × 1 mm^3) cut from hot-pressed pellets. Each sample ingot was mounted on a copper holder, which incorporates a small heater (120 Ω strain gauge) located close to one end of the sample. The copper holder is attached to the hot stage of a closed-cycle refrigerator (DE-202, Advanced Research Systems), which is connected to a Lakeshore LS-331 temperature controller. Two 50μm copper wires were attached to the ends of the sample using silver paint and connections made to a Keithley 2182A nanovoltmeter. Two Au: 0.07% Fe vs. chromel thermocouples were placed at the hot and cold ends, and connected to a second Lakeshore LS-331 temperature controller.

[1] A.C. Larson and R.B. von Dreele, General Structure Analysis System, Los Alamos Laboratory, 1994.
[2] Hiramatsu, H.; Yanagi, H.; Kamiya, T.; Ueda, K.; Hirano, M.; Hosono, H.; *Chem. Mater*. 2008, **20**, 326.

The Seebeck coefficient at a given temperature was determined by applying a temperature gradient, ΔT, across the sample and measuring the corresponding thermal voltage, ΔV. The slope of the line, $\Delta V/\Delta T$, was used to determine the Seebeck coefficient.

High-temperature electrical conductivity and Seebeck coefficient

The electrical conductivity σ and Seebeck coefficient S were measured by using an Ulvac-Riko ZEM 3 system from 300K to 825K under partial Helium pressure. According to the manufacturer, the uncertainty of the Seebeck coefficient and electrical conductivity is ±7%.

Thermal conductivity

The thermal conductivity over the temperature range $100 \leq T/°C \leq 400$, was measured using a commercial instrument (Anter FL3000), which applies the laser flash method, on hot-pressed pellets. This instrument determines both the thermal diffusivity (α) and the heat capacity (Cp) of the sample, and the thermal conductivity (κ) is calculated from the relationship:

$$\kappa = \alpha \, Cp \, \rho$$

where ρ is the sample density. For the determination of the heat capacity, side-by-side testing of a reference material, PyroceramTM 9606, was carried out.

According to the instrument manufacturer, the uncertainty of the thermal diffusivity measurements is ±3% and for heat capacity measurements is ±6%. Considering the uncertainties of α, Cp and ρ, we estimate that the overall uncertainty of the thermal conductivity will be around ±7%.

We estimate that the combined uncertainty for all measurements used for the determination of ZT is *ca.* 15%.

2. **Rietveld refinements and powder X-ray diffraction analysis**

(a)

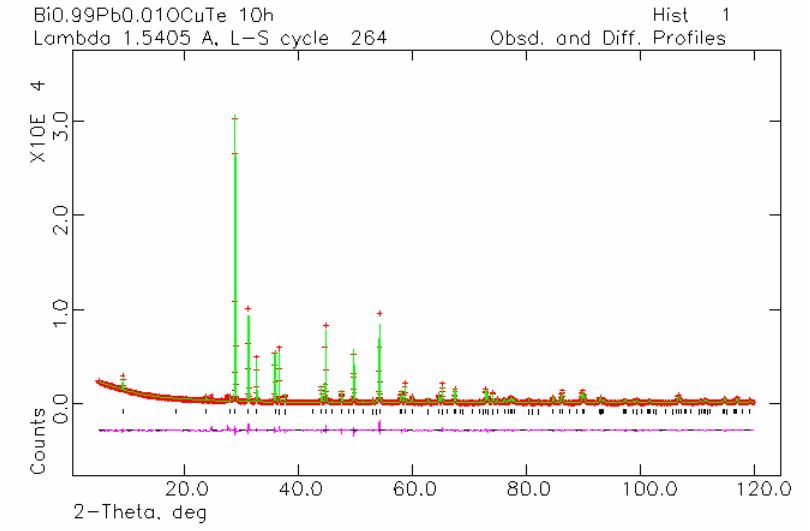

(b)

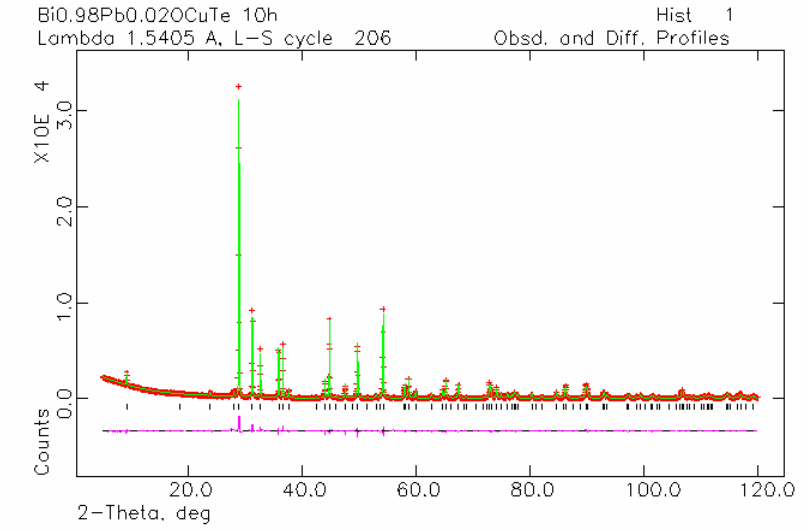

(c)

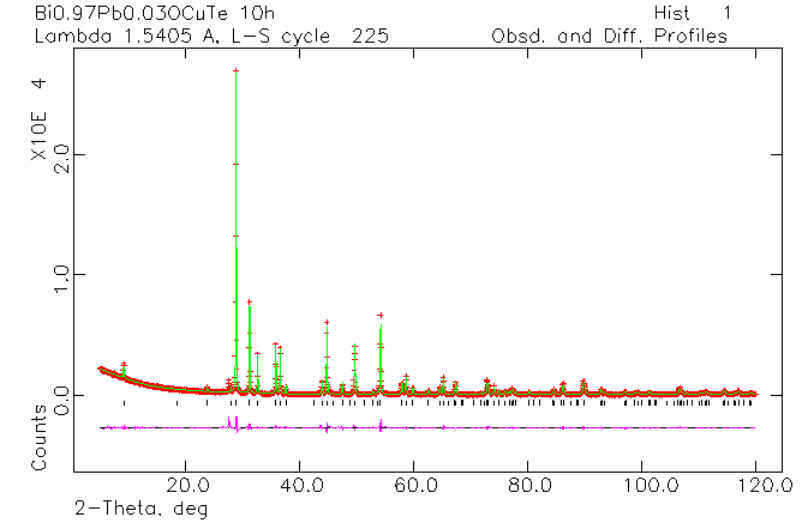

(d)

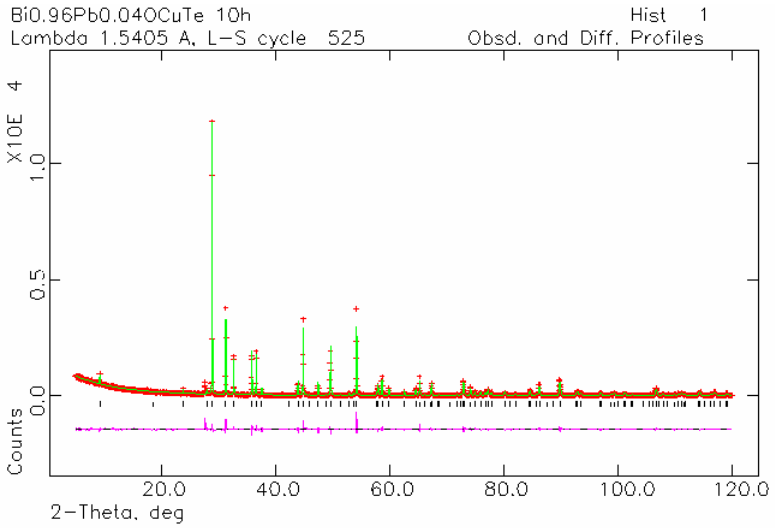
Bi0.96Pb0.04OCuTe 10h
Hist 1
Lambda 1.5405 A, L-S cycle 525
Obsd. and Diff. Profiles
X10E 4
1.0
0.5
0.0
Counts
20.0
40.0
60.0
80.0
100.0
120.0
2-Theta, deg

(e)

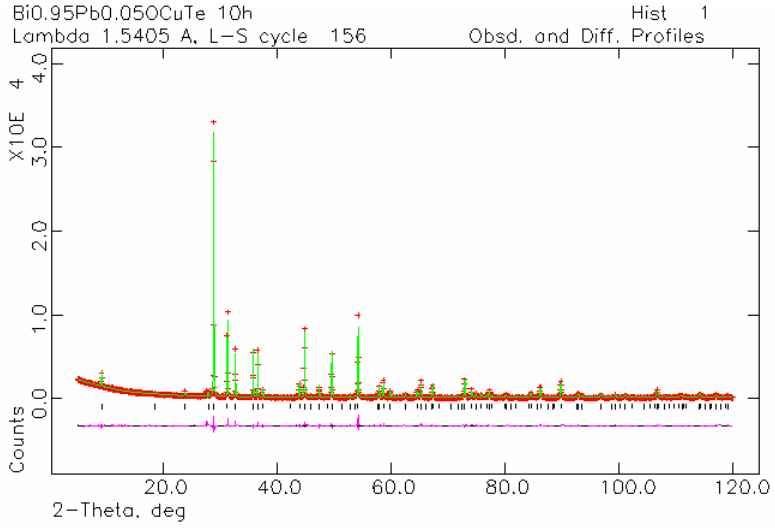
Bi0.95Pb0.05OCuTe 10h
Hist 1
Lambda 1.5405 A, L-S cycle 156
Obsd. and Diff. Profiles
X10E 4
4.0
3.0
2.0
1.0
0.0
Counts
20.0
40.0
60.0
80.0
100.0
120.0
2-Theta, deg

(f)

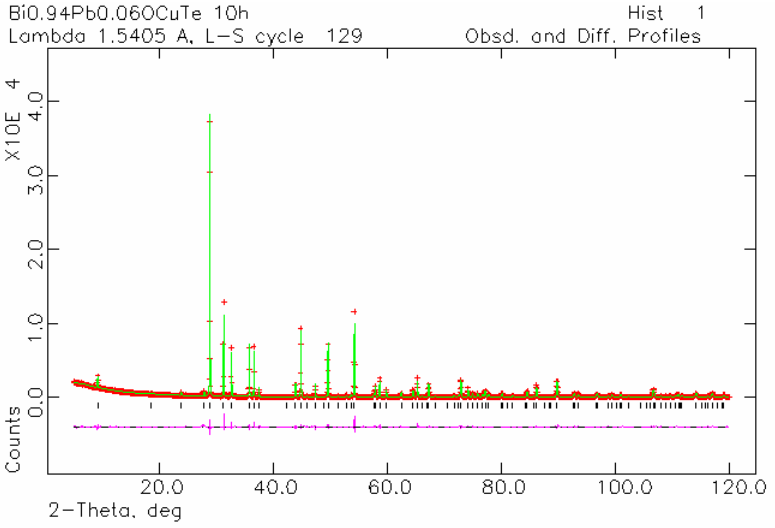
Bi0.94Pb0.06OCuTe 10h
Hist 1
Lambda 1.5405 A, L-S cycle 129
Obsd. and Diff. Profiles
X10E 4
4.0
3.0
2.0
1.0
0.0
Counts
20.0
40.0
60.0
80.0
100.0
120.0
2-Theta, deg

(g)

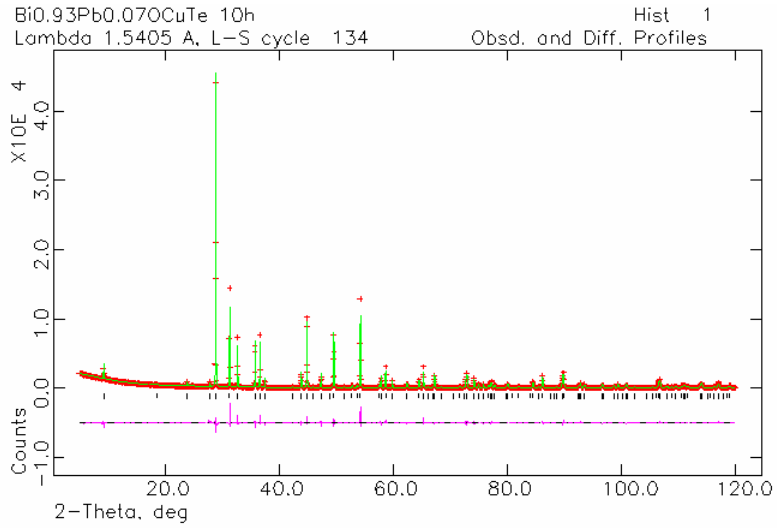

(h)

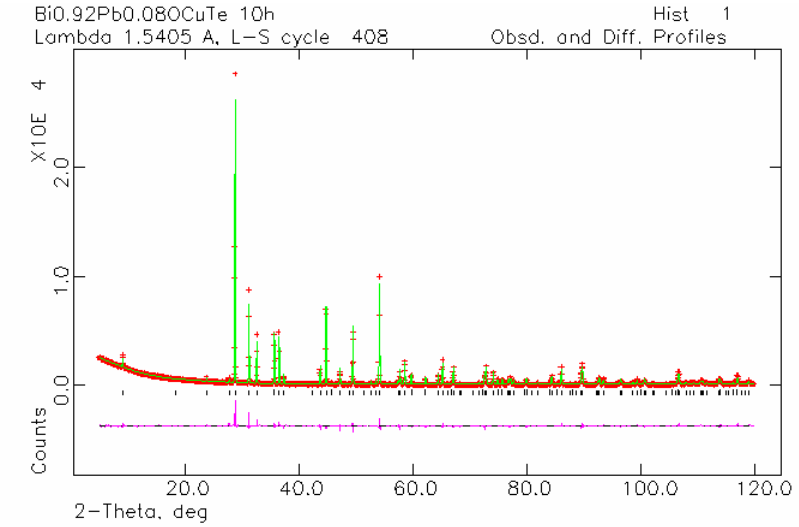

Figure S1. Rietveld refinements using power diffraction data for $Bi_{1-x}Pb_xOCuTe$ ($0.01 \leq x \leq 0.08$).

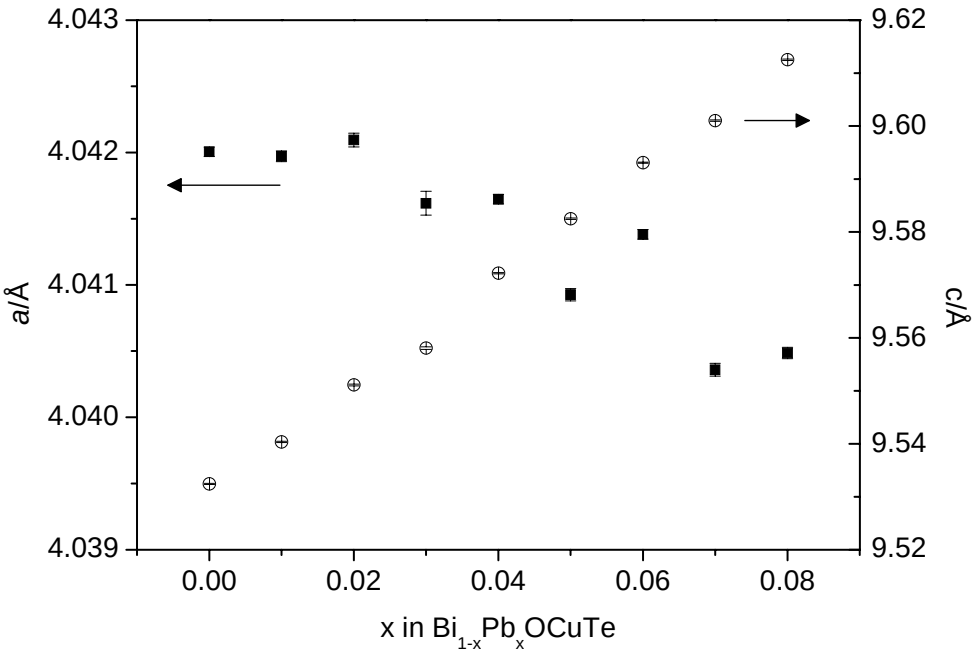

Figure S2. Lattice parameters for $Bi_{1-x}Pb_xOCuTe$ ($0 \le x \le 0.08$).

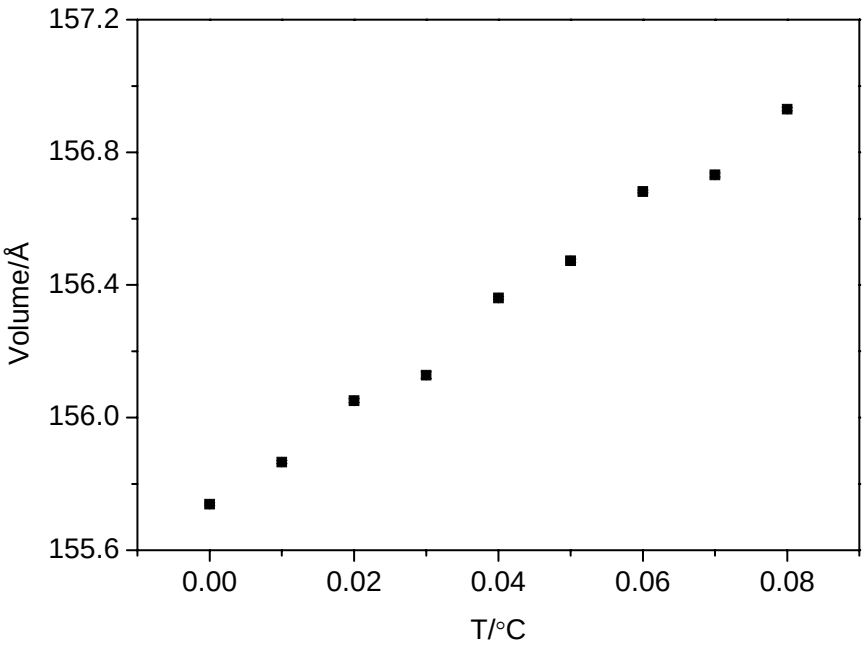

Figure S3. Unit cell volume for $Bi_{1-x}Pb_xOCuTe$ ($0 \le x \le 0.08$)

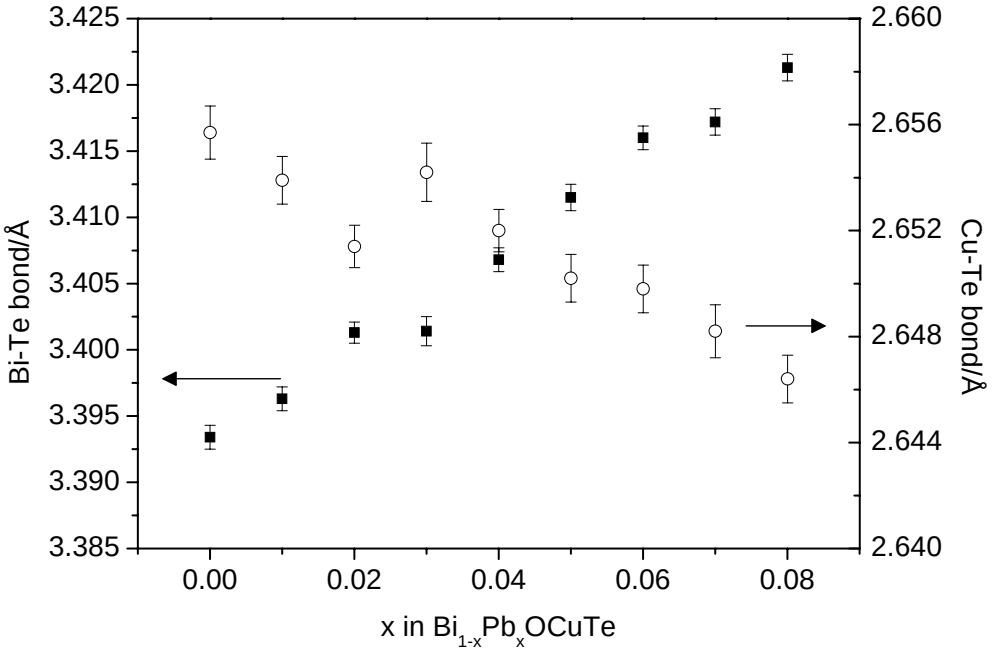

Figure S4. Bi-Te and Cu-Te bond lengths for $Bi_{1-x}Pb_xOCuTe$ ($0 \le x \le 0.08$).

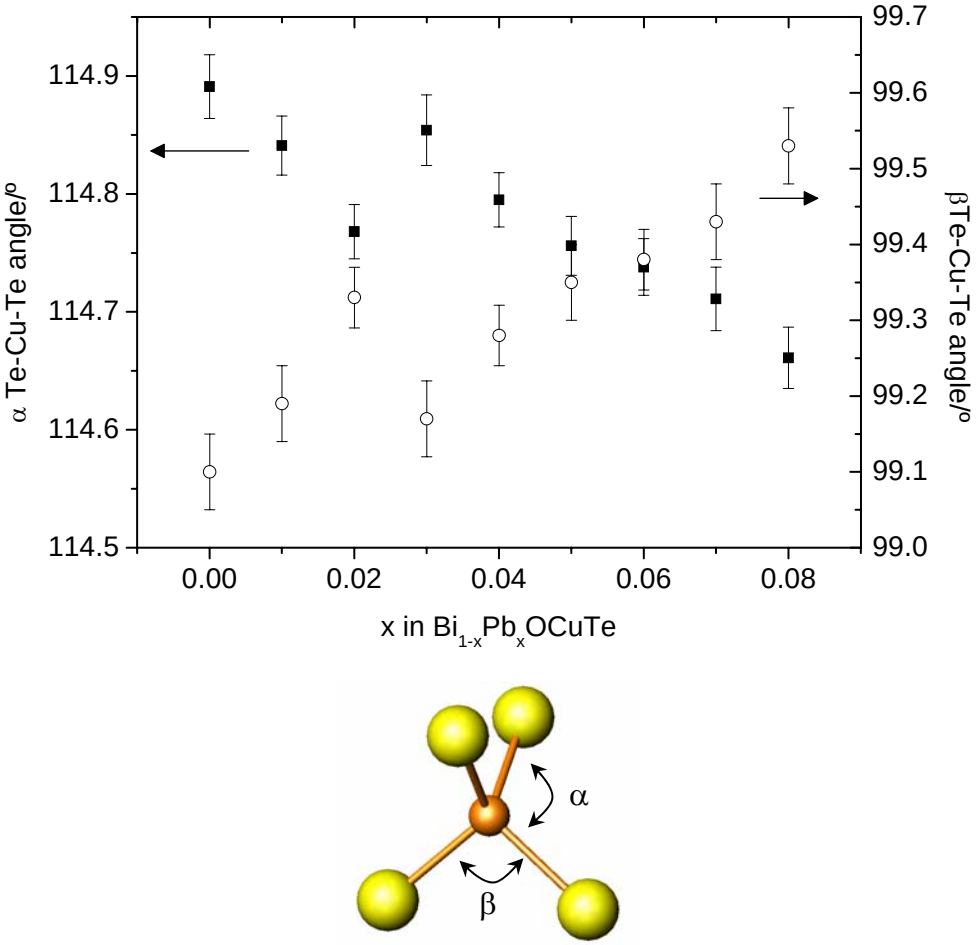

Figure S5. Te-Cu-Te bond angles for $Bi_{1-x}Pb_xOCuTe$ ($0 \le x \le 0.08$).

Table S1. Final refined parameters for $Bi_{1-x}Pb_xOCuTe$ ($0 \leq x \leq 0.08$). Site occupancy factors for Bi and Pb were fixed at the stoichiometric composition.

		x in $Bi_{1-x}Pb_xOCuTe$								
		0.0	0.01	0.02	0.03	0.04	0.05	0.06	0.07	0.08
	a/Å	4.04200(4)	4.04197(4)	4.04209(5)	4.04162(9)	4.04164(4)	4.04093(5)	4.04138(4)	4.04036(5)	4.04049(4)
	c/Å	9.5324(1)	9.5403(1)	9.5511(2)	9.5580(2)	9.5722(1)	9.5825(1)	9.5931(1)	9.6010(1)	9.6125(1)
Bi/Pb[a]	*z*	0.1274(1)	0.1274(1)	0.1273(1)	0.1270(1)	0.1269(1)	0.1265(1)	0.1262(1)	0.1264(1)	0.1264(1)
	$B/Å^2$	0.50(2)	0.61(2)	1.17(2)	1.05(3)	1.01(4)	1.05(2)	1.02(2)	0.76(2)	0.86(2)
O[b]	$B/Å^2$	0.6(3)	0.4(3)	1.6(3)	1.0(4)	1.4(3)	1.3(3)	1.2(3)	0.9(4)	2.0(4)
Cu[c]	$B/Å^2$	1.02(8)	1.11(8)	1.85(8)	1.53(9)	1.49(8)	1.52(8)	1.47(8)	1.27(8)	1.54(8)
Te[a]	*z*	0.6808(2)	0.6803(1)	0.6797(1)	0.6800(2)	0.6794(1)	0.6790(1)	0.6786(1)	0.6783(2)	0.6778(2)
	$B/Å^2$	0.37(3)	0.53(4)	0.99(3)	0.90(4)	0.79(3)	0.82(3)	0.81(3)	0.56(4)	0.71(4)
R_{wp}/%		12.4	9.5	9.3	10.4	14.1	9.6	10.0	11.8	11.1

[a]Bi/Pb and Te on 2(*c*) (0,0,1/2); [b]O on 2(*a*) (3/4,1/4,0); [c]Cu on 2(*b*) (3/4,1/4,1/2).

3. Physical properties

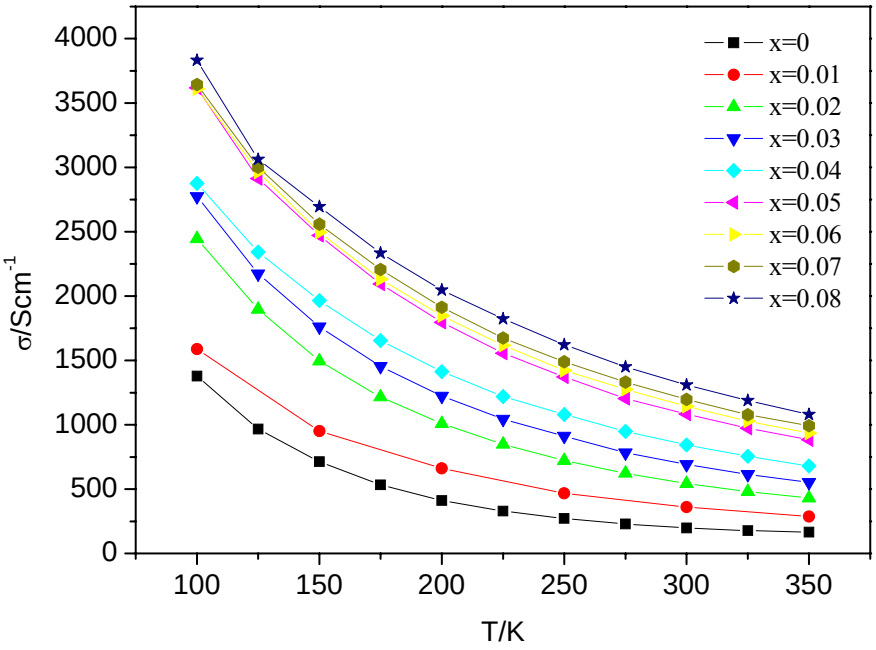

Figure S6. Electrical conductivity for $Bi_{1-x}Pb_xOCuTe$ ($0 \le x \le 0.08$) at low temperatures.

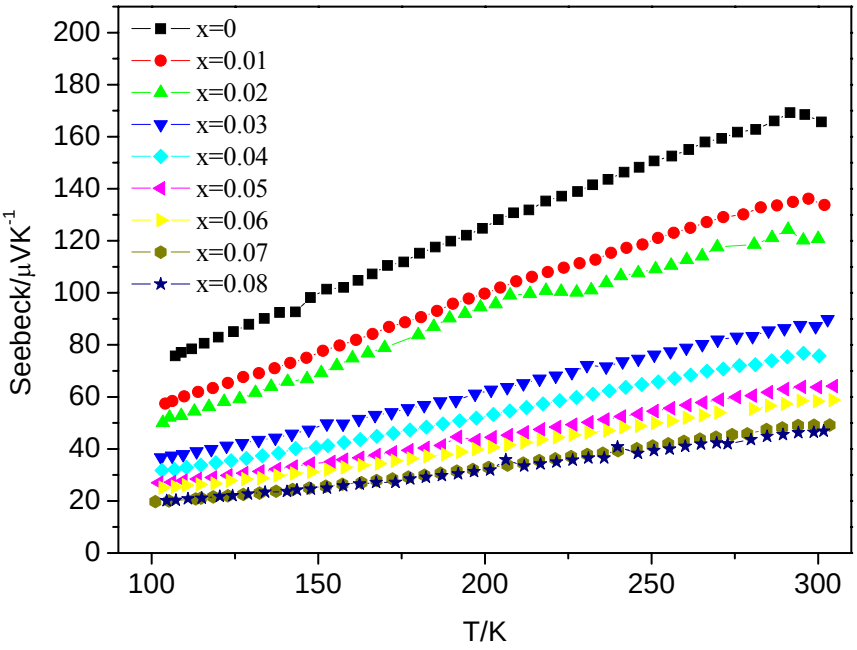

Figure S7. Seebeck coefficient for $Bi_{1-x}Pb_xOCuTe$ ($0 \le x \le 0.08$) at low temperatures.

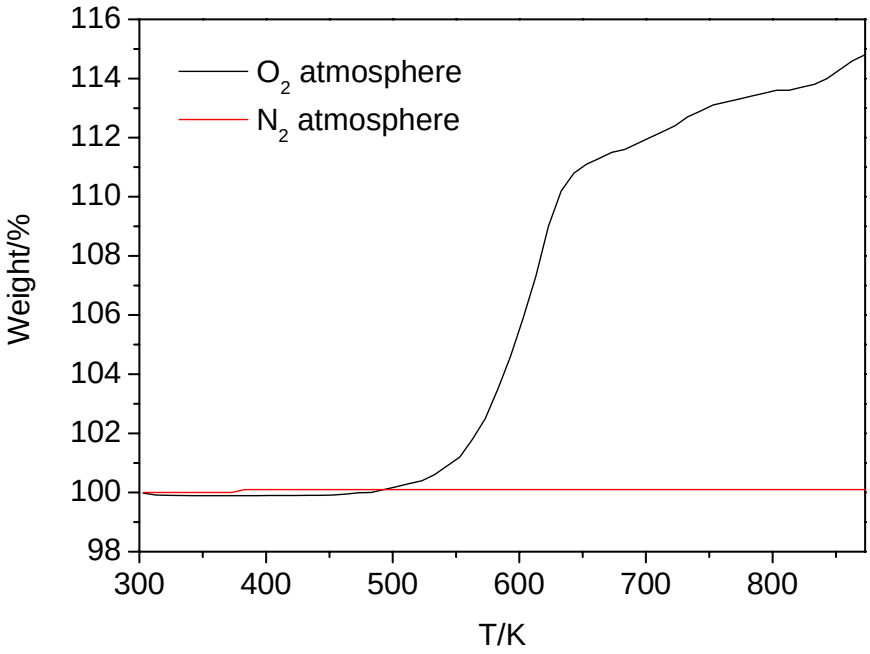

Figure S8. Thermogravimetric analysis of BiOCuTe under O_2 and N_2 atmospheres.

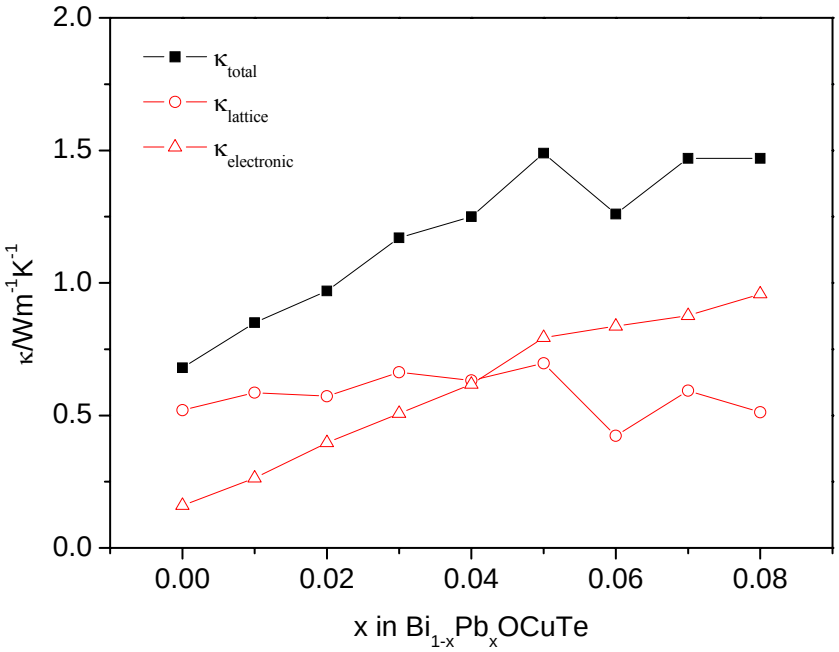

Figure S9. Estimated lattice and electronic thermal conductivities for $Bi_{1-x}Pb_xOCuTe$ ($0 \leq x \leq 0.08$) at 373 K.